PCCP

Accepted Manuscript

ROYAL SOCIETY OF CHEMISTRY

www.rsc.org/pccp

PCCP

RSCPublishing

COMMUNICATION

The Control of Pt and Ru Nanoparticle Size on High Surface Area Supports

Cite this: DOI: 10.1039/xoxxoooooox

Qiuli Liu, Upendra A. Joshi, Kevin Über and John R. Regalbuto*

Received ooth January 2012,
Accepted ooth January 2012

DOI: 10.1039/xoxxoooooox

www.rsc.org/

Supported Ru and Pt nanoparticles are synthesized by the method of Strong Electrostatic Adsorption and subsequently treated under different steaming-reduction conditions to achieve series of catalysts with controlled particle sizes, ranging from 1 to 8 nm. While in case of oxidation-reduction condition, only Pt yields particles from 2.5 to 8 nm and Ru loss observed. Both Ru and Pt sinter faster in air than hydrogen. This methodology allows for the control of particle size using a "production-scalable" catalyst synthesis method which can be applied to high surface area supports with common metal precursors.

Supported noble metal catalysts have been widely used in chemical and energy production as well as environmental protection.[1] Bridging the areas of energy production and environmental protection, the upgrading of bio-oil to transportation grade fuels has attracted much attention in recent years. Unlike metal sulphides, supported metal catalysts do not require the addition of sulfur to maintain stability. The metal used as hydrogenation catalysts are not prone to coking as are zeolites. Prior studies have shown that supported metal hydrogenation catalysts have the ability to hydrogenate and deoxygenate phenolic compounds.[2-4] For example, supported metal catalysts (Pt/SiO_2, Ru/SiO_2, Pt/Al_2O_3, Ru/Al_2O_3, Pt/C, Ru/C, etc.) can be used to upgrade bio-oil via hydrodeoxygenation for production of traditional refinery-ready hydrocarbon feedstock. The effect of metal, solvent and mass-transfer on catalytic hydroprocessing of *p*-cresol as a model compound has been investigated by Wan et. al.[5] Similarly, Foster et. al.[6] studied the effect of acid functionalized support and metal function for *m*-cresol hydrodeoxygenation. Very recently, Lercher group investigated the importance of Ni nanoparticle size and distribution on the hydrodeoxygentation of microalgae oil.[7]

The most widely used procedure to synthesize supported metal catalysts is dry impregnation (DI, also known as incipient wetness impregnation) due to its simplicity. In this method, precursor solution is impregnated into the support in the amount just necessary to fill the pore volume. The resulting thick slurry is dried and the final metal catalysts are obtained after removal of precursor ligands and reduction of the metal by a variety of thermal and chemical treatments. However, in dry impregnation there is no control over the interaction of the metal precursor with the support surface and agglomeration of metal often occurs during drying and/or reduction steps.

The number of active metal sites is often described in terms of dispersion, or the ratio of metal sites existing at nanoparticle surfaces, divided by the total number of metal atoms. Metal nanoparticles with 1 nm are considered to have 100% dispersion. This is desirable in many cases; however, many reactions exist for which larger particle sizes give higher overall activity by virtue of greater numbers of certain sites such as terrace sites present only in larger particles. The size dependence of many chemical reactions has not been studied in a systematic way (for example, there have been no reports on the systematic control of noble metal particle size and its effect on the catalytic hydrodeoxygenation of bio-oil or any model bio-oil compounds); thus it is important to have a method to produce a smoothly varying set of particle sizes which can be synthesized over the same support.

That is the purpose of the present work. We will employ the method of Strong Electrostatic Adsorption (SEA), which can be used to synthesize the ultra-small metal nanoparticles; from this starting point, thermal and chemical treatments will be applied to sinter the particles to larger and larger sizes. In this way, series of catalysts with well-controlled ranges of particle sizes can be prepared over commercially viable, high surface area supports using common metal precursors. The widely used silica support is used in this study and this method can be applied to other supports as well.

SEA is coulombic in nature and can be achieved with precise pH control.[8] Oxide surfaces terminate in hydroxyl groups which can be protonated or deprotonated as a function of solution pH. At these conditions the support can electrostatically adsorb oppositely charged metal precursors. Anion precursors will adsorb over a protonated surface below the PZC, similarly, cations will adsorb over a deprotonated surface above the PZC.

The hypothesis behind the SEA approach to catalyst preparation is that monolayer adsorption of metal complexes via strong electrostatic adsorption can lead to small metal particles when the complexes are reduced.[9] Our research efforts have been focused on the synthesis of noble metal catalysts using strong electrostatic adsorption.[10-13] SEA has been demonstrated to synthesize ultra-small (1-2 nm) metal nanoparticles on various metal oxide and carbon

supports, but precise size control for higher range particles has not yet been demonstrated.

We utilize strong electrostatic adsorption to synthesize ultra-small (about 1 nm) Pt and Ru metal nanoparticles over amorphous SiO_2 and SBA-15 supports followed by thermochemical sintering to achieve series of sizes. The hydrodeoxygenation (HDO) of *p*-cresol has been investigated using as a probe reaction to demonstrate the effect of particle size on reactivity

The detailed experimental procedure is explained in the supporting information. Briefly, SiO_2 (Aerosil-380) was obtained from Evonik and SBA-15 was prepared as per a previous report.[14] Ruthenium hexaammine chloride ($[Ru(NH_3)_6]Cl_3$, 99.9%) and platinum tetraammine chloride ($[Pt(NH_3)_4]Cl_2$, 99.9%) obtained from Aldrich and designated as RuHA and PTA respectively were used as ruthenium and platinum precursors. Inductively coupled plasma optical emission spectrometry (ICP-OES) was used to determine metal uptake. All catalysts were synthesized around the optimal pH followed by temperature programmed reduction (TPR) to determine the reduction temperatures. Catalysts were characterized by X-ray diffraction (XRD) and scanning transmission electron microscopy (STEM) to determine metal particle sizes. The catalytic hydrodeoxygenation was performed in a batch reactor at 300°C with 300 PSIG partial pressure of hydrogen for 2 hrs using water as a solvent. The final product is a two phase mixture, water phase was washed with dichloromethane to recover product and mixed with oil phase. Dichloromethane is used as a solvent, and only one phase was analysed by GC with biphenyl as an internal standard.

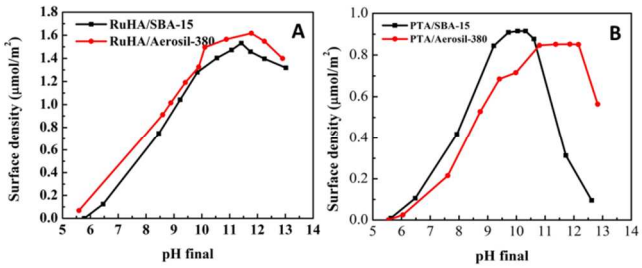

Fig 1. Metal surface density vs final pH of solution at 1000 m^2/L: A) RuHA; B) PTA on SBA-15 and Aerosil-380.

As described in the Supplementary information, the PZCs of SBA-15 and Aerosil-380 were determined to be 4.4 and 4.5, respectively. Thus, cation metal complexes such as platinum tetraammine chloride (PTA) and ruthenium hexamine chloride (RuHA) were chosen as precursor. PTA and RuHA strongly adsorb onto the deprotonated silica surface above its PZC, and an uptake survey can be used to locate the pH of strongest electrostatic adsorption. Figure 1 represents uptake surveys of RuHA/SBA-15, RuHA/Aerosil-380, PTA/SBA-15, and PTA/Aerosil-380 for 1000 m^2/L surface loading (m^2 of support per litre of precursor solution) and 200 ppm metal as a function of final pH of solution. The metal uptake is reported as surface density, in μmol/m^2. SBA-15 and Aerosil 380 both follow essentially the same trend and are similar to silica[13]. No adsorption occurred below pH 6 as hydroxyl groups are not deprotonated sufficiently. Volcano-shaped plots are observed in the range of pH 6 to pH 13. As pH increases the adsorption of RuHA increase and reaches maximum surface density of 1.6 μmol/m^2; while in case of PTA maximum surface density of 0.9 μmol/m^2 is observed (Figure 1B). In case of RuHA, the maximum adsorption occurs at pH 11.4. The retardation of adsorption process occurs at pH extremes, caused by high ionic strength, which decreases adsorption equilibrium constant[13]. The same trends are seen in all the other uptake surveys. For the same precursor, similar maximum adsorption can be obtained on different silica supports at the same surface loading.

The limit of metal uptake is thought to be steric; a monolayer is limited to a closed-packed arrangement of complexes which retain one or two hydration sheaths. The maximum uptake of PTA is 0.9 μmol/m^2 or 1 complex/ 2 nm^2, which corresponds to the retention of two hydration sheaths by the square planar PTA complex[13]. It appears that the octahedral RuHA complex, which adsorbs at 1.6 μmol/m^2 or 1 complex/nm^2, retains only one hydration sheath.

Temperature program reduction (TPR) was performed on all filtered and dried SEA samples to determine the temperature of reduction of the metal complexes to metal. The TPR profile (in supporting information Figure S1 A) shows two peak for the RuHA complex. The reduction of Ru^{4+} to Ru^0 occurred at around 180°C whereas Ru^{3+} reduces to metallic Ru^0 at 300~350°C. Hence all RuHA/SiO_2 catalysts were reduced at 300°C to obtain metallic Ru particles on SBA-15 and Aerosil 380 silica. Two reduction peaks were also observed for PTA samples, one at 280°C and another at 350~400°C (Figure S1B in supporting information). Goguet et. al.[15] systematically studied the decomposition of $[Pt(NH_3)_4(OH)_2]_n$ complex on SiO_2 and suggested that the decomposition steps involve an intermediate complex which anchors to SiO_2 strongly during drying process and then decomposes to Pt^0. All PTA/SiO_2 catalysts were reduced at 350°C.

Scanning transmission electron microscope (STEM) was used to obtain high-angle annular dark-field (Z-contrast) images for each sample. Figure 2 shows typical images for 9.7 wt% Ru and 5.4 wt% Pt particles deposited on SBA-15 prepared via SEA at monolayer adsorption.

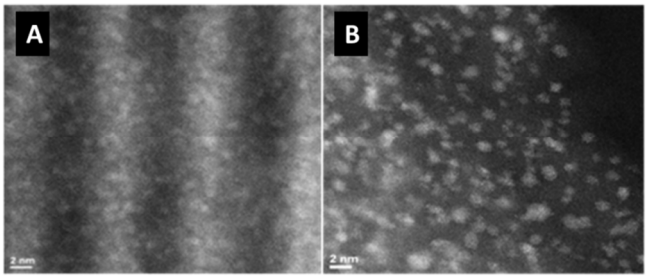

Fig 2. Representative STEM images and corresponding particle size distribution of a) Ru and b) Pt on SBA-15; bar scale 2 nm.

The hexagonal pore structure of SBA-15 is seen in some orientations of the sample as dark and bright contrast channels as in Figure 2A. Figure 2B shows a side view of the hexagonal channels of the Pt/SBA-15 sample. Metal particle sizes of the reduced catalysts prepared by SEA show very narrow size distribution throughout the SBA-15 pore channels. The average particle size for 9.7 wt% Ru/SBA-15 is 1.1 nm ± 0.2 nm, and that of the 5.4 wt% Pt/SBA-15 is also 1.3 nm ± 0.3 nm (Fig S4 in supporting information).

XRD analysis was performed with a high sensitivity Si slit detector (D/teX ultra, Rigaku) allowing detection of particles as small as about 1 nm. The patterns for Ru/SBA-15 and Pt/SBA-15 are shown in Figures 3A and 3B respectively. The broad peak around 21 degrees 2θ is due to amorphous silica. The metal nanoparticles are below the detection limit of XRD, consistent with STEM results in Figure 2. No significant increase in particle size has been observed for the Ru/SBA-15 samples reduced at 500 °C for 2 hrs and 700 °C for 2 hrs. The Ru/SBA-15 samples reduced at 900 °C for 2 hrs yields about 1.4 nm Ru particles. Similar thermal treatment carried out for Pt/SBA-15 is shown in Figure 3B. The average particle sizes do not change much up to reduction temperatures of 700°C. Sintering of Pt on SBA-15starts at 800°C, and at 900°C samples

show mixed platinum-silicon phases ($Pt_{64}Si_{36}$ and Pt_2Si, Fig 3B pattern d).

As there was no significant sintering of metallic Ru and Pt up to 700°C and 900°, respectively, harsher conditions were required. A steaming-reduction process was employed using hydrogen saturated with water vapor for various times. Based on the results of Figure 3, 900 and 800°C reduction temperatures were selected for Ru/SBA-15

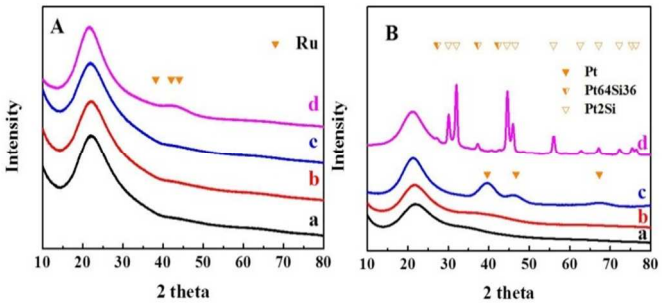

Fig 3. The XRD pattern showing the effect of heat treatment on the A) Ru/SBA-15, all reduction proceeded 2 hrs at a) 300 °C, b) 500 °C, c) 700 °C and d) 900 °C; and B) Pt/SBA-15 catalysts, reduction proceeded at a) 350 °C-2 hrs, b) 700 °C-2 hrs, c) 800°C-2 hrs and d) 900 °C-3 hrs No significant increase observed up to 700 °C in both cases.

and Pt/SBA-15 respectively. Figure 4 displays the XRD patterns for the two metals at various steaming reduction times. As the reduction time increases a gradual increase in particle size is observed. For Ru/SBA-15, steaming reduction at 900°C for 1 h gives particles of *ca.* 1.4 nm. At 12 hours, size is 2.8 nm, and at 24 hrs, particles of 4.5 nm are obtained as shown in Table 1.

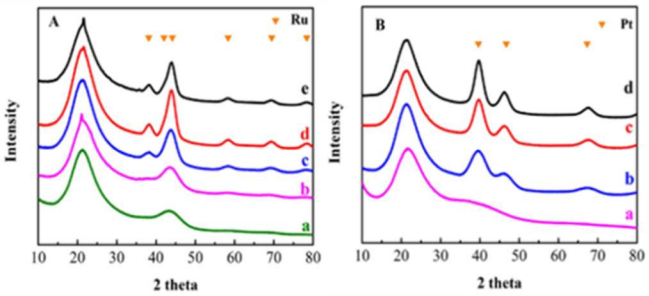

Fig 4. The effect of steaming-reduction time on particle size of A) Ru/SBA-15 at 900 °C, a) 1.4 nm with 1 hr SR, b) 1.8 nm with 3 hrs SR, c) 3.0 nm with 6 hrs SR, d) 3.8 nm with 12 hrs SR and e) 4.5 nm with 24 hrs SR; and B) Pt/SBA-15 at 800 °C, a) ~1.0 nm with 2 hrs (700 °C) SR, b) 2.0 nm with 2hrs SR, c) 2.8 nm with 10 hrs SR and d) 3.3 nm with 16 hrs SR; orange triangle shows the position of Ru and Pt peaks respectively.

A similar steaming-reduction process was performed at 800°C on Pt/SBA-15 with time varied from 2 to 16 hrs. This yielded particle sizes ranging from 1 nm to 3.3 nm (Table 1). The broad peak observed at 2θ = 38.72° in pattern a of Figure 4B can be deconvoluted as Pt_3O_4 (211) (35.92°) and Pt (111) (39.76°) (Fig S5 in supporting information). It appears that the smallest Pt particles (which are about 1.0 nm speculatively) can be substantially oxidized at room temperature. Small particles of Pt have been shown by past EXAFS analysis to oxidize at ambient conditions; the current study indicates that the phase is Pt_3O_4.

These results demonstrate that the size of noble metal particles supported on silica can be tailored with time and temperature of steam reduction. However, these harsh conditions affected the pore structure of the SBA-15 support as revealed by surface area measurements before and after the reduction treatment. Table 1 summarizes the BET surface area analysis. The pure SBA-15 support used with Ru had a surface area of about 486 m^2/g with uniform pore size around 5 nm (Fig S6, S7 in supporting information). For Ru/SBA-15 catalysts, the 900°C steaming-reduction rapidly (one hour) diminished the surface area to 200 m^2/g or below and the pore structure was completely destroyed. The SBA-15 employed for Pt had an original surface area of 340 m^2/g and did not collapse so significantly (about 15%) at the 800°C steaming-reduction treatment for Pt.

HAADF-STEM images of Ru particles following steam reduction treatment at 24h in Fig 5 clearly show Ru sintering. The particle size (see Fig S8 in supporting information) of 5.1 ± 0.6 nm nm was consistent with the XRD size estimate (4.5 mm) obtained from Fig 4A. In many areas Ru particles smaller than 1 nm were observed to coexist with much larger particles as shown in Fig 5B. This is consistent with the Ostwald ripening mechanism of sintering as found recently by the Datye group for Ni particle sintering in hydrogen and moisture.[16,17] In the present case, metal sintering is complicated by support sintering, even though the silica supports calcined at 900°C for 6 hrs had an intact pore structure (see BET results of Fig S6 and STEM images in figure S7 of supporting information). STEM images of the 24 hrs steam-reduced samples (not shown) revealed no hexagonal pore structure. The moisture content was thus responsible for the instability of the silica phase at 900°C.

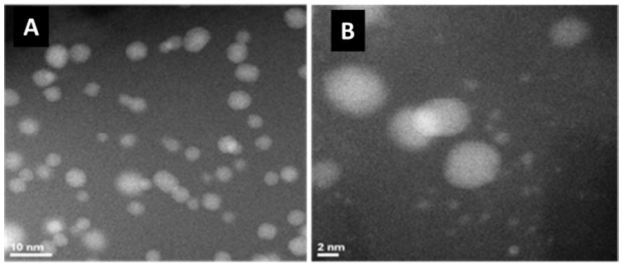

Fig 5. HAADF-STEM images of Ru/SBA-15 after steaming reduction at 900 °C/24 h.

Table 1. Properties of Ru/SBA-15 and Pt/SBA-15 catalysts.[a]

Ru/SBA-15			Pt/SBA-15		
Time (h)	Particle size (nm)[b]	SA (m^2/g)[c]	Time (h)	Particle size (nm)[b]	SA (m^2/g)[c]
0[d]	1.1	468	0[d]	1.3	340
1	1.4	155	2	2.0	NA[e]
12	3.8	207	10	2.8	NA[e]
24	4.5	201	16	3.3	292

[a]Steaming-reduction carried out at 900 °C for Ru/SBA-15 and 800 °C for Pt/SBA-15, [b]From XRD, [c]From BET, [d]Pure support as received, no steaming treatment. [e]NA = Not available

For catalytic applications the collapse of pore structure is undesirable and so a method to sinter the well dispersed metal phase at lower temperature was devised, based on an earlier study which indicated that calcining Pt ammine precursors (in air) forms a

sintered intermediate Pt oxide phase and ultimately lowers the dispersion of reduced nanoparticles[10].

Our attempts to sinter Ru particles by oxidization were largely unsuccessful. When calcined at 300°C or above, significant Ru loss was apparent by its deposition on the crucible (dark coloration) containing the catalyst. Of the Ru which remains on the support, large (32 nm) RuO_2 particles form, and convert to 8 nm Ru metal particles when reduced. This temperature is lower than what is normally though to induce volatilization[18,19], although Ragaini et. al.[19] do point out that volatilization is a function of Ru loading and our loading (9.7 wt%) is relatively high.

With a 200°C oxidization, no RuO_2 phase was observed until 5 hrs, and after reduction these particles were 2.5 nm. Any longer oxidization at 200°C resulted in Ru loss. Attempts at reduction-oxidization-reduction cycles were also unsuccessful at preventing Ru volatilization, as were similar experiments conducted with the amorphous Aerosil 380 silica support. Thus in general it is difficult to sinter Ru by oxidization without a significant loss of Ru, though there may be a narrow temperature window in which this can be done for a particular Ru loading.

Results with oxidization of Pt, on the other hand, were successful. With oxidation-reduction treatments on Pt/SBA-15 at 200°C for several hours, platinum oxide peaks are below the detection limit of XRD. Oxidation at a higher temperature of 300°C for 3 hrs revealed platinum oxide particles which can be reduced at 180°C (determined from TPR of the calcined catalyst in Figure S3) to give 2.5 nm Pt particles (Fig 6A pattern a). Oxidization at successively higher temperatures yielded Pt particle sizes of 4.0, 4.8, 6.1, and 8.0 nm Pt particles on SBA-15 (Figure 6A, b-e).

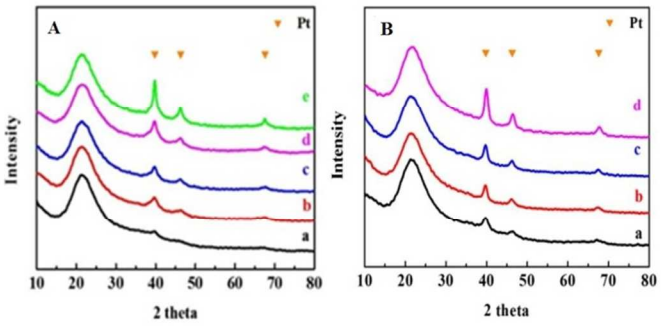

Fig 6. XRD patterns of 180°C reduced A) Pt/SBA-15 catalysts after oxidation for a) 300 °C for 3 hrs (2.5 nm), b) 400 °C for 3 hrs (4.0 nm), c) 450 °C for 3 hrs (5.0 nm), d) 450 °C for 4 hrs (6.1 nm) and e) 500 °C for 3 hrs (8.0 nm) ; B) Pt/Aerosil-380 oxidized at a) 300 °C for 1 hr (3.5 nm), b) 300 °C for 3hrs (4.5 nm), c) 300 °C for 4 hrs (6.0 nm) and d) 400 °C for 3 hrs (8.0 nm).

A similar range of sizes was prepared over Aerosil-380; particles of 3.5, 4.5, 6.0, and 8.0 nm are shown in Figure 6B. Starting particle size was 1.3 ± 0.3 nm with some oxidation, as in Figure 2B. The oxidization temperatures required to achieve a particular particle size are less than those for the corresponding SBA-15–supported sample, implying that the SBA-15 better anchors Pt against sintering than amorphous silica. No metal loss was observed in case of Pt/SBA-15 and Pt/Aerosil-380 catalysts.

The hydrodeoxygenation (HDO) of *p*-cresol has been studied in a batch reactor using three of the Pt/SBA-15 catalysts of sizes 1.3, 2.5, and 8 nm. All reaction experiments were carried out at 300 °C with hydrogen partial pressure 300 PSIG for 2 hrs duration. As seen in Figure 7 the overall conversion for all catalysts is about 20%. The selectivity of the products depends upon the pathway of the reaction. The product distribution shows a predominance of 4-methylcyclohexanol, suggesting that *p*-cresol undergoes ring hydrogenation. The selectivity for a desired high octane aromatic, toluene, is 5-8% while second largest product is 4-methylcyclohexanone. A hydrogenation-dehydration reaction mechanism is likely the predominant pathway on noble metal catalysts rather than direct hydrogenolysis of C-O bond.[20] Foster et al.[6] studied the influence of support acid-base characterization on the selectivity and rate of *m*-cresol conversion for a number of SiO_2 and Al_2O_3 modified supports. Similarly, Wang et. al.[21] studied the effect of acidity and mesoporous structure to the HDO of *m*-cresol and found that strong support acidity has high HDO activity. As SBA-15 silica used in this study has low acidity the overall activity is low compared to the study Pt/Al_2O_3 and Pt/C studied by Wan et. al.[5] Detail study is underway to investigate the effect of support on the activity in our laboratory and results will be followed in separate report.

The turn over frequency (TOF) is calculated using the average particle size from XRD and is plotted versus particle size in Figure 8B. Provided that the activity measurements are free of mass transfer limitations, the increase of the TOF by a factor of 5 for the larger nanoparticles suggests that the reaction is structure sensitive. The reaction study is to be detailed in another work; here we only wish to demonstrate the usefulness of a simply prepared series of particle sizes in learning about the reaction.

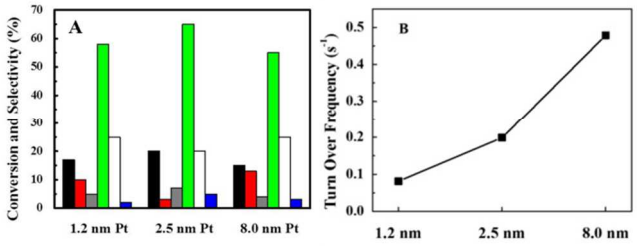

Fig 7. Hydrodeoxygenation of p-cresol over 3.2 wt% Pt/SBA-15 catalysts with varying particle size of Pt. Reaction conditions: solvent = water; temperature = 300 °C, H_2 partial pressure = 300 PSIG, time = 2h. Legend: (*black*) p-cresol conversion, (*red*) unaccounted products, (*grey*) toluene selectivity, (*green*) 4-methylcyclohexanol selectivity, (*white*) 4-methylcyclohexanone selectivity, (*blue*) methylcyclohexane selectivity.

In conclusion, we have synthesized supported Pt and Ru nanoparticle size series using strong electrostatic adsorption procedure followed by two thermochemical treatments. A high temperature steam reduction yielded particles from 1.1 nm to 4.5 nm. However the steaming reduction procedure significantly affects the pore structure of SBA-15 and drastically reduces the surface area. A lower temperature oxidation – reduction procedure better preserves the support and gives a good size distribution of Pt nanoparticles, but cannot be effectively used with Ru due to ruthenium oxide volatilization. The HDO of *p*-cresol over Pt/SBA-15 shows high selectivity towards 4-methylcyclohexanol, with larger particles (8.0 nm) exhibiting a five times higher TOF than the smallest (1.3 nm) particles.

Acknowledgement

This work was supported by USDA-NIFA grant 59-1935-3-001.

Notes and References

Department of Chemical Engineering, University of South Carolina, 301 Main Street Columbia, SC 29208, USA.
Email: regalbuj@cec.sc.edu

† Electronic Supplementary Information (ESI) available: Experimental section, supporting TPR data, STEM images, particle size distribution and XRD deconvolution of platinum oxide. See DOI: 10.1039/c000000x/

1 J. M. Campelo, D. Luna, R. Luque, J. M. Marinas, A. A. Romero, *ChemSusChem*., 2009, 2, 18.
2 Z. He, X. Wang, *Catal. Sus. Energy*., 2013, **1**, 28.
3 P. M. Mortensen, J-D, Grunwaldt, P. A. Jensen, A. D. Jensen, ACS Catal., 2013, **3**, 1774.
4 T. Wang, G. Mpourmpakis, W. W. Lonergan, D. G. Vlachos, J. G. Chen, *Phys. Chem. Chem. Phys*., 2013, **15**, 12156.
5 H. Wan, R. V. Chaudhari, B. Subramaniam, *Top. Catal.,* 2012, **55**, 129.
6 A. J. Foster, P. T. M. Do, R. F. Lobo, *Top. Catal.* 2012, **55**, 118.
7 W. Song, C. Zhao, J. A. Lercher, *Chem. Eur. J.* 2013, **19**, 9833.
8 J. P. Brunelle, *Pure Appl. Chem.,* 1978, **50**, 1211.
9 J. Park, J. R. Regalbuto, *J. Colloid Interface Sci*., 1995, **175**, 239.
10 J. T. Miller, A. J. Kropf, M. Schreier, J. R. Regalbuto, *J. Catal*., 2004, **225**, 203.
11 J. R. Regalbuto, *Surface and Nanomolecular Catalysis*, Taylor and Francis/CRC Press, Borca Raton, FL, 2006, p.161.
12 X. Zhu, H-R, Cho, M. Pasupong, J. R. Regalbuto, *ACS Catal.,* 2013, **3**, 625.
13 L. Jiao, J. R. Regalbuto, *J. Catal*., 2008, **260**, 329.
14 D. Zhao, J. Feng, Q. Huo, N. Melosh, G. H. Fredickson, B. F. Chmelka, G. D. Stucky, *Science*, 1998, **279**, 548.
15 A. Goguet, D. Schweich, J. –P. Candy, *J. Catal.* 2003, **220**, 280.
16 S. R. Challa, A. T. Delariva, T. W. Hansen, S. Helveg, J. Sehested, P. L. Hansen, F. Garzon, A. K. Datye, *J. Am. Chem. Soc.* 2011, **133**, 20672.
17 T. W. Hansen, A. T. Delariva, S. R. Challa, A. K. Datye, *Acc. Chem. Res.* 2013, **46**, 1720.
18 W. Zou, R. D. Gonzalez, *J. Catal.* 1992, **133**, 202.
19 V. Ragaini, C. Pirola, S. Vitali, G. Bonura, C. Cannilla, F. Frusteri, *Catal. Lett.* 2012, **142**, 1452.
20 F. E. Massoth, P. Politzer, M. C. Concha, J. S. Murray, J. Jakowski, J. Simons, J. Phys. Chem B., 2006, 110, 14283.
21 Y. Wang, J. Wu, S. Wang, RSC Adv. 2013, 3, 12635.